PERGAMON

International Journal of Solids and Structures 40 (2003) 5335–5352

INTERNATIONAL JOURNAL OF SOLIDS and STRUCTURES

www.elsevier.com/locate/ijsolstr

Three-dimensional exact analysis of a simply supported functionally gradient piezoelectric plate

Z. Zhong *, E.T. Shang

Key Laboratory of Solid Mechanics of MOE, Department of Engineering Mechanics and Technology, Tongji University, 1239 Siping Road, Shanghai 200092, PR China

Received 6 November 2002; received in revised form 23 April 2003

Abstract

An exact three-dimensional analysis is presented for a functionally gradient piezoelectric material rectangular plate that is simply supported and grounded along its four edges. The state equations of the functionally gradient piezoelectric material are developed based on the state space approach. Assuming that the mechanical and electric properties of the material have the same exponent-law dependence on the thickness-coordinate, we obtain an exact three-dimensional solution of the coupling electroelastic fields in the plate under mechanical, and electric loading on the upper and lower surfaces of the plate. The influences of the different functionally gradient material properties on the structural response of the plate to the mechanical and electric stimuli are then studied through examples.

Keywords: Functionally gradient piezoelectric material; Electroelastic coupling; Rectangular plate; State space approach; Exact solution

1. Introduction

Piezoelectric materials have been widely used as actuators and sensors in smart and adaptive systems due to their intrinsic coupling of mechanical and electric fields (Gandhi and Thompson, 1992; Rao and Sunar, 1994). In order to achieve large deformation, piezoelectric actuators are often constructed as bimorph or stacked form, by bonding together two piezoelectric ceramic sheets in strip or plate forms. While these designs can provide large displacement, they have great disadvantages. The bonding of two different piezoelectric materials or identical piezoelectric materials with different poling directions will cause severe interfacial stress concentration, and trigger the initiation and propagation of micro-cracks near the interface which may lead to failure of the devices. Such drawbacks reduce the reliability and life span of piezoelectric devices and limit their applications.

* Corresponding author. Tel.: +86-21-65982483; fax: +86-21-65981138.
E-mail address: zhongk@online.sh.cn (Z. Zhong).

0020-7683/$ - see front matter © 2003 Elsevier Ltd. All rights reserved.
doi:10.1016/S0020-7683(03)00288-9

In order to overcome the drawbacks of conventional piezoelectric bimorphs, a new kind of piezoelectric materials, named functionally gradient piezoelectric materials (FGPMs), has been developed (Zhu and Meng, 1995; Wu et al., 1996; Shelley et al., 1999). FGPM is a kind of piezoelectric material with material composition and properties varying continuously along certain directions. The piezoelectric devices can be entirely made of FGPM or use FGPM as a transit interlayer between different piezoelectric materials. The advantage of this new kind of materials is that no discernible internal boundaries exist and failures from interfacial stress concentrations developed in conventional bimorphs can be avoided. FGPM actuators can thus produce large displacements while minimizing the internal stress concentrations, which will greatly improve the reliability and life of piezoelectric actuators. Nowadays, advancement of modern materials processing technology has enabled the fabrication of materials with arbitrary compositional gradient in a controlled fashion. The relationship between the material compositional gradient and the electromechanical responses of FGPM structures is very important in the design of FGPM devices. This research subject is so new that only a few results can be found in the literature. Most of the available results on the structural analysis of FGPM plate were based on a laminated structure scheme by which the FGPM plate was approximately modeled as a laminated structure. For example, this scheme was employed by Liu and Tani (1994) to study the wave propagation in FGPM plates, by Chen and Ding (2002) to analyze the free vibration of FGPM rectangular plates. Other related works include: Lim and He (2001) obtained an exact solution of a compositionally graded piezoelectric layer under uniform stretch, bending and twisting; Reddy and Cheng (2001) obtained a three-dimensional solution of smart functionally gradient plate; Li and Weng (2002a,b), Hu et al. (2002), Jin and Zhong (2002) studied the problems of an antiplane crack in functionally gradient piezoelectric materials.

The objective of this work is to present an exact solution of a simply supported functionally gradient piezoelectric rectangular plate based on three-dimensional electroelasticity theory. The obtained exact solution could serve as a benchmark result to assess other approximate methodologies or as a basis for establishing simplified FGPM plate theories.

2. Formulation

Consider a FGPM rectangular plate of uniform thickness h, as shown in Fig. 1. Introduce a Cartesian coordinate system $\{x_i\}$ $(i = 1, 2, 3)$ such that the bottom and top surfaces of the undeformed plate lie in the plane $x_3 = 0$ and $x_3 = h$. The lengths of the edges of the plate in x_1- and x_2-direction are respectively denoted by a and b. Throughout the paper, the Einsteinian summation convention over repeated indices of tensor components is used, with Latin indices ranging from 1 to 3 while Greek indices over 1 and 2.

In the absence of body forces and electric charge density, the field equations of elastic equilibrium and Gauss' law of electrostatics are (Tiersten, 1969; Maugin, 1988)

$$\sigma_{ij,j} = 0 \qquad D_{i,i} = 0 \tag{1}$$

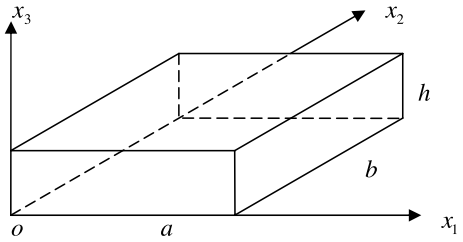

Fig. 1. A schematic of the rectangular plate.

where σ_{ij} is the stress tensor, D_i the electric displacement vector, a comma denotes partial differentiation with respect to the coordinate x_i.

The strain ε_{ij} and the electric field E_i are related to the elastic displacements u_i and the electric potential ϕ through the following relations:

$$\varepsilon_{ij} = \tfrac{1}{2}(u_{i,j} + u_{j,i}) \qquad E_i = -\phi_{,i} \tag{2}$$

The constitutive relations of FGPM are

$$\sigma_{ij} = c_{ijkl}\varepsilon_{kl} - e_{kij}E_k \qquad D_i = e_{ikl}\varepsilon_{kl} + \lambda_{ik}E_k \tag{3}$$

where c_{ijkl}, e_{ikl}, λ_{ik} are the elastic stiffness tensor, the piezoelectric tensor and the dielectric tensor, with the interchange symmetries $c_{ijkl} = c_{jikl} = c_{ijlk} = c_{klij}$, $e_{kij} = e_{kji}$, $\lambda_{ik} = \lambda_{ki}$. Unlike in a homogeneous piezoelectric material, c_{ijkl}, e_{ikl}, λ_{ik} are now functions of the coordinates x_i ($i = 1, 2, 3$). In most real cases, the material property parameters are varied continuously only in one direction. In the present study, we consider the material properties having the following exponential distributions

$$c_{ijkl} = c^0_{ijkl}\,\mathrm{e}^{\alpha(x_3/h)} \qquad e_{ikl} = e^0_{ikl}\,\mathrm{e}^{\alpha(x_3/h)} \qquad \lambda_{ik} = \lambda^0_{ik}\,\mathrm{e}^{\alpha(x_3/h)} \tag{4}$$

where c^0_{ijkl}, e^0_{ikl} and λ^0_{ik} are the values at the plane $x_3 = 0$, α is the material property gradient index which can be determined by the values of the material properties at the planes, $x_3 = 0$ and $x_3 = h$, i.e.

$$\alpha = \ln c^h_{ijkl} - \ln c^0_{ijkl} = \ln e^h_{ikl} - \ln e^0_{ikl} = \ln \lambda^h_{ik} - \ln \lambda^0_{ik} \tag{5}$$

The assumption that the material properties vary exponentially with spatial position is not only simple for mathematical treatment, it also provides some essential features of functionally gradient materials. Therefore, it was employed by many researchers to model the elastic or thermoelastic behaviors of functionally gradient material (e.g., Erdogan, 1985; Delale and Erdogan, 1988; Noda and Jin, 1993; Gu and Asaro, 1997; among others).

Next we will consider an orthotropic functionally gradient material, for which the nonzero components of the elastic stiffness tensor, the piezoelectric tensor and the dielectric tensor are c_{1111}, c_{2222}, c_{3333}, c_{1122}, c_{1133}, c_{2233}, c_{2323}, c_{1313}, c_{1212}, e_{311}, e_{322}, e_{333}, e_{113}, e_{223}, λ_{11}, λ_{22}, λ_{33}. Following the process of state space approach used in piezoelectricity (Lee and Jiang, 1996; Ding et al., 1999; Cheng et al., 2000), the following relations in matrix form can be obtained from (1)–(3):

$$\partial_3 \begin{bmatrix} \mathbf{\Pi} \\ \mathbf{\Gamma} \end{bmatrix} = \begin{bmatrix} \mathbf{0} & \mathbf{A} \\ \mathbf{B} & \mathbf{0} \end{bmatrix} \begin{bmatrix} \mathbf{\Pi} \\ \mathbf{\Gamma} \end{bmatrix} \tag{6}$$

$$\begin{bmatrix} \mathbf{\Lambda} \\ \mathbf{T} \end{bmatrix} = \begin{bmatrix} \mathbf{0} & \mathbf{C} \\ \mathbf{D} & \mathbf{0} \end{bmatrix} \begin{bmatrix} \mathbf{\Pi} \\ \mathbf{\Gamma} \end{bmatrix} \tag{7}$$

where $\partial_i \equiv \partial/\partial x_i$ ($i = 1, 2, 3$), and

$$\mathbf{\Pi} = [\, u_1 \quad u_2 \quad \sigma_{33} \quad D_3 \,]^{\mathrm{T}} \qquad \mathbf{\Gamma} = [\, \sigma_{13} \quad \sigma_{23} \quad u_3 \quad \phi \,]^{\mathrm{T}} \tag{8}$$

$$\mathbf{\Lambda} = [\, D_1 \quad D_2 \,]^{\mathrm{T}} \qquad \mathbf{T} = [\, \sigma_{11} \quad \sigma_{22} \quad \sigma_{12} \,]^{\mathrm{T}} \tag{9}$$

The operator matrices **A**, **B**, **C**, **D** contain the in-plane differential operators ∂_1 and ∂_2, and depend on x_3 only through the material moduli:

$$\mathbf{A} = \begin{bmatrix} c^{-1}_{1313} & 0 & -\partial_1 & -k_{11}\partial_1 \\ 0 & c^{-1}_{2323} & -\partial_2 & -k_{12}\partial_2 \\ -\partial_1 & -\partial_2 & 0 & 0 \\ -k_{11}\partial_1 & -k_{12}\partial_2 & 0 & k_{21}\partial_1^2 + k_{22}\partial_2^2 \end{bmatrix} \tag{10}$$

$$\mathbf{B} = \begin{bmatrix} -k_{31}\partial_1^2 - c_{1212}\partial_2^2 & k_8\partial_1\partial_2 & -k_4\partial_1 & -k_5\partial_1 \\ k_8\partial_1\partial_2 & -c_{1212}\partial_1^2 - k_{33}\partial_2^2 & -k_6\partial_2 & -k_7\partial_2 \\ -k_4\partial_1 & -k_6\partial_2 & k_0\lambda_{33} & k_0 e_{333} \\ -k_5\partial_1 & -k_7\partial_2 & k_0 e_{333} & -k_0 c_{3333} \end{bmatrix} \tag{11}$$

$$\mathbf{C} = \begin{bmatrix} k_{11} & 0 & 0 & -k_{21}\partial_1 \\ 0 & k_{12} & 0 & -k_{22}\partial_2 \end{bmatrix} \tag{12}$$

$$\mathbf{D} = \begin{bmatrix} k_{31}\partial_1 & k_{32}\partial_2 & k_4 & k_5 \\ k_{32}\partial_1 & k_{33}\partial_2 & k_6 & k_7 \\ c_{1212}\partial_2 & c_{1212}\partial_1 & 0 & 0 \end{bmatrix} \tag{13}$$

where

$$k_0 = \frac{1}{c_{3333}\lambda_{33} + e_{333}^2} \qquad k_{11} = \frac{e_{113}}{c_{1313}} \qquad k_{12} = \frac{e_{223}}{c_{2323}}$$

$$k_{21} = \frac{e_{113}^2}{c_{1313}} + \lambda_{11} \qquad k_{22} = \frac{e_{223}^2}{c_{2323}} + \lambda_{22}$$

$$k_{31} = c_{1111} - k_0(c_{1133}^2\lambda_{33} + 2c_{1133}e_{311}e_{333} - e_{311}^2 c_{3333})$$

$$k_{32} = c_{1122} - k_0(c_{1133}c_{2233}\lambda_{33} + c_{1133}e_{322}e_{333} + c_{2233}e_{311}e_{333} - c_{3333}e_{311}e_{322})$$

$$k_{33} = c_{2222} - k_0(c_{2233}^2\lambda_{33} + 2c_{2233}e_{322}e_{333} - e_{322}^2 c_{3333})$$

$$k_4 = k_0(c_{1133}\lambda_{33} + e_{311}e_{333}) \qquad k_5 = k_0(c_{1133}e_{333} - c_{3333}e_{311})$$

$$k_6 = k_0(c_{2233}\lambda_{33} + e_{322}e_{333}) \qquad k_7 = k_0(c_{2233}e_{333} - c_{3333}e_{322})$$

$$k_8 = k_4 c_{2233} + k_5 e_{322} - c_{1122} - c_{1212}$$

For a rectangular plate that is simply supported and grounded on all four edges, the edge conditions are given by

$$\begin{aligned} &\sigma_{11} = u_2 = u_3 = \phi = 0 \quad \text{at } x_1 = 0 \text{ and } a \\ &\sigma_{22} = u_1 = u_3 = \phi = 0 \quad \text{at } x_2 = 0 \text{ and } b \end{aligned} \tag{14}$$

Boundary conditions at the top and bottom surfaces are

at $x_3 = 0$ (bottom surface):

$$\begin{aligned} &\sigma_{13} = X^-(x_1, x_2) \qquad \sigma_{23} = Y^-(x_1, x_2) \qquad \sigma_{33} = Z^-(x_1, x_2) \\ &D_3 = D^-(x_1, x_2) \qquad (\text{or } \Phi = \Phi^-(x_1, x_2)) \end{aligned} \tag{15}$$

and at $x_3 = h$ (top surface):

$$\begin{aligned} &\sigma_{13} = X^+(x_1, x_2) \qquad \sigma_{23} = Y^+(x_1, x_2) \qquad \sigma_{33} = Z^+(x_1, x_2) \\ &D_3 = D^+(x_1, x_2) \qquad (\text{or } \Phi = \Phi^+(x_1, x_2)) \end{aligned} \tag{16}$$

3. Solution

The state variables that satisfy the boundary condition (14) can be assumed as

$$\mathbf{\Pi} = \begin{bmatrix} u_1 \\ u_2 \\ \sigma_{33} \\ D_3 \end{bmatrix} = \sum_{m=1}^{\infty}\sum_{n=1}^{\infty} \begin{bmatrix} U_{mn}(x_3)\cos\left(\frac{m\pi x_1}{a}\right)\sin\left(\frac{n\pi x_2}{b}\right) \\ V_{mn}(x_3)\sin\left(\frac{m\pi x_1}{a}\right)\cos\left(\frac{n\pi x_2}{b}\right) \\ \mathrm{e}^{\alpha(x_3/h)}Z_{mn}(x_3)\sin\left(\frac{m\pi x_1}{a}\right)\sin\left(\frac{n\pi x_2}{b}\right) \\ \mathrm{e}^{\alpha(x_3/h)}D_{mn}(x_3)\sin\left(\frac{m\pi x_1}{a}\right)\sin\left(\frac{n\pi x_2}{b}\right) \end{bmatrix} \tag{17}$$

$$\mathbf{\Gamma} = \begin{bmatrix} \sigma_{13} \\ \sigma_{23} \\ u_3 \\ \phi \end{bmatrix} = \sum_{m=1}^{\infty}\sum_{n=1}^{\infty} \begin{bmatrix} \mathrm{e}^{\alpha(x_3/h)}X_{mn}(x_3)\cos\left(\frac{m\pi x_1}{a}\right)\sin\left(\frac{n\pi x_2}{b}\right) \\ \mathrm{e}^{\alpha(x_3/h)}Y_{mn}(x_3)\sin\left(\frac{m\pi x_1}{a}\right)\cos\left(\frac{n\pi x_2}{b}\right) \\ W_{mn}(x_3)\sin\left(\frac{m\pi x_1}{a}\right)\sin\left(\frac{n\pi x_2}{b}\right) \\ \Phi_{mn}(x_3)\sin\left(\frac{m\pi x_1}{a}\right)\sin\left(\frac{n\pi x_2}{b}\right) \end{bmatrix} \tag{18}$$

Substituting (17) and (18) into (6), we obtain the following matrix equation

$$\frac{\partial \mathbf{M}_{mn}}{\partial x_3} = \mathbf{K}_{mn}\mathbf{M}_{mn} \tag{19}$$

where

$$\mathbf{M}_{mn} = [\, U_{mn} \quad V_{mn} \quad Z_{mn} \quad D_{mn} \quad X_{mn} \quad Y_{mn} \quad W_{mn} \quad \Phi_{mn} \,]^{\mathrm{T}} \tag{20}$$

and

$$\mathbf{K}_{mn} = \begin{bmatrix} \mathbf{K}_1^{mn} & \mathbf{K}_3^{mn} \\ \mathbf{K}_4^{mn} & \mathbf{K}_2^{mn} \end{bmatrix} \tag{21}$$

with $\mathbf{K}_1^{mn}$, $\mathbf{K}_2^{mn}$, $\mathbf{K}_3^{mn}$ and $\mathbf{K}_4^{mn}$ being given as

$$\mathbf{K}_1^{mn} = \begin{bmatrix} 0 & 0 & 0 & 0 \\ 0 & 0 & 0 & 0 \\ 0 & 0 & -\frac{\alpha}{h} & 0 \\ 0 & 0 & 0 & -\frac{\alpha}{h} \end{bmatrix} \qquad \mathbf{K}_2^{mn} = \begin{bmatrix} -\frac{\alpha}{h} & 0 & 0 & 0 \\ 0 & -\frac{\alpha}{h} & 0 & 0 \\ 0 & 0 & 0 & 0 \\ 0 & 0 & 0 & 0 \end{bmatrix}$$

$$\mathbf{K}_3^{mn} = \begin{bmatrix} \frac{1}{c^0_{1313}} & 0 & -\frac{m\pi}{a} & -k^0_{11}\frac{m\pi}{a} \\ 0 & \frac{1}{c^0_{2323}} & -\frac{n\pi}{b} & -k^0_{12}\frac{n\pi}{b} \\ \frac{m\pi}{a} & \frac{n\pi}{b} & 0 & 0 \\ k^0_{11}\frac{m\pi}{a} & k^0_{12}\frac{n\pi}{b} & 0 & -k^0_{21}\left(\frac{m\pi}{a}\right)^2 - k^0_{22}\left(\frac{n\pi}{b}\right)^2 \end{bmatrix}$$

$$\mathbf{K}_4^{mn} = \begin{bmatrix} k_{31}^0\left(\frac{m\pi}{a}\right)^2 + c_{1212}^0\left(\frac{n\pi}{b}\right)^2 & -k_8^0\frac{m\pi}{a}\frac{n\pi}{b} & -k_4^0\frac{m\pi}{a} & -k_5^0\frac{m\pi}{a} \\ -k_8^0\frac{m\pi}{a}\frac{n\pi}{b} & c_{1212}^0\left(\frac{m\pi}{a}\right)^2 + k_{33}^0\left(\frac{n\pi}{b}\right)^2 & -k_6^0\frac{n\pi}{b} & -k_7^0\frac{n\pi}{b} \\ k_4^0\frac{m\pi}{a} & k_6^0\frac{n\pi}{b} & \lambda_{33}^0 k_0 & e_{33}^0 k_0 \\ k_5^0\frac{m\pi}{a} & k_7^0\frac{n\pi}{b} & e_{33}^0 k_0 & -c_{33}^0 k_0 \end{bmatrix} \tag{22}$$

with

$$k_0^0 = \frac{1}{c_{3333}^0\lambda_{33}^0 + (e_{333}^0)^2} \qquad k_{11}^0 = \frac{e_{113}^0}{c_{1313}^0} \qquad k_{12} = \frac{e_{223}^0}{c_{2323}^0}$$

$$k_{21}^0 = \frac{(e_{113}^0)^2}{c_{1313}^0} + \lambda_{11}^0 \qquad k_{22}^0 = \frac{(e_{223}^0)^2}{c_{2323}^0} + \lambda_{22}^0$$

$$k_{31}^0 = c_{1111}^0 - k_0^0[(c_{1133}^0)^2\lambda_{33} + 2c_{1133}^0 e_{311}^0 e_{333}^0 - (e_{311}^0)^2 c_{3333}^0]$$

$$k_{32}^0 = c_{1122}^0 - k_0^0(c_{1133}^0 c_{2233}^0\lambda_{33}^0 + c_{1133}^0 e_{322}^0 e_{333}^0 + c_{2233}^0 e_{311}^0 e_{333}^0 - c_{3333}^0 e_{311}^0 e_{322}^0)$$

$$k_{33}^0 = c_{2222}^0 - k_0^0\lfloor(c_{2233}^0)^2\lambda_{33}^0 + 2c_{2233}^0 e_{322}^0 e_{333}^0 - (e_{322}^0)^2 c_{3333}^0\rfloor$$

$$k_4^0 = k_0^0(c_{1133}^0\lambda_{33}^0 + e_{311}^0 e_{333}^0) \qquad k_5^0 = k_0^0(c_{1133}^0 e_{333}^0 - c_{3333}^0 e_{311}^0)$$

$$k_6^0 = k_0^0(c_{2233}^0\lambda_{33}^0 + e_{322}^0 e_{333}^0) \qquad k_7^0 = k_0^0(c_{2233}^0 e_{333}^0 - c_{3333}^0 e_{322}^0)$$

$$k_8^0 = k_4^0 c_{2233}^0 + k_5^0 e_{322}^0 - c_{1122}^0 - c_{1212}^0$$

The solution to Eq. (19) can be written as (Gantmacher, 1960)

$$\mathbf{M}_{mn}(x_3) = \mathbf{T}(x_3)\mathbf{M}_{mn}(\mathbf{0}) \tag{23}$$

where $\mathbf{T}(x_3) = e^{\mathbf{K}_{mn}x_3}$ is called a transfer matrix, which can be further expanded into a matrix polynomial from the Cayley–Hamilton theorem, as follows:

$$\mathbf{T}(x_3) = e^{\mathbf{K}_{mn}x_3} = \sum_{p=0}^{7} a_p(x_3)\mathbf{K}_{mn}^p \tag{24}$$

Assuming that the 8×8 matrix $\mathbf{K}_{mn}$ takes distinct eigenvalues $\eta_1, \ldots, \eta_8$, which is valid for most cases of anisotropic materials, we have

$$e^{\eta_i x_3} = \sum_{p=0}^{7} a_p(x_3)\eta_i^p \quad (i = 1, \ldots, 8) \tag{25}$$

(25) forms a set of eight linear algebraic equations for eight unknown coefficients $a_p(x_3)$, $p = 0, 1, \ldots, 7$. Once these coefficients are obtained, the transfer matrix $\mathbf{T}(x_3)$ can readily be determined from Eq. (24). Then, from (23), we can get

$$\mathbf{M}_{mn}(h) = \mathbf{T}(h)\mathbf{M}_{mn}(\mathbf{0}) \tag{26}$$

or

$$\begin{bmatrix} U_{mn}(h) \\ V_{mn}(h) \\ Z_{mn}(h) \\ D_{mn}(h) \\ X_{mn}(h) \\ Y_{mn}(h) \\ W_{mn}(h) \\ \Phi_{mn}(h) \end{bmatrix} = \begin{bmatrix} T_{11}(h) & T_{12}(h) & T_{13}(h) & T_{14}(h) & T_{15}(h) & T_{16}(h) & T_{17}(h) & T_{18}(h) \\ T_{21}(h) & T_{22}(h) & T_{23}(h) & T_{24}(h) & T_{25}(h) & T_{26}(h) & T_{27}(h) & T_{28}(h) \\ T_{31}(h) & T_{32}(h) & T_{33}(h) & T_{34}(h) & T_{35}(h) & T_{36}(h) & T_{37}(h) & T_{38}(h) \\ T_{41}(h) & T_{42}(h) & T_{43}(h) & T_{44}(h) & T_{45}(h) & T_{46}(h) & T_{47}(h) & T_{48}(h) \\ T_{51}(h) & T_{52}(h) & T_{53}(h) & T_{54}(h) & T_{55}(h) & T_{56}(h) & T_{57}(h) & T_{58}(h) \\ T_{61}(h) & T_{62}(h) & T_{63}(h) & T_{64}(h) & T_{65}(h) & T_{66}(h) & T_{67}(h) & T_{68}(h) \\ T_{71}(h) & T_{72}(h) & T_{73}(h) & T_{74}(h) & T_{75}(h) & T_{76}(h) & T_{77}(h) & T_{78}(h) \\ T_{81}(h) & T_{82}(h) & T_{83}(h) & T_{84}(h) & T_{85}(h) & T_{86}(h) & T_{87}(h) & T_{88}(h) \end{bmatrix} \begin{bmatrix} U_{mn}(0) \\ V_{mn}(0) \\ Z_{mn}(0) \\ D_{mn}(0) \\ X_{mn}(0) \\ Y_{mn}(0) \\ W_{mn}(0) \\ \Phi_{mn}(0) \end{bmatrix} \tag{27}$$

The mechanical and electric loads on the top and bottom surfaces of the plate (see boundary conditions (15) and (16)) can be further expanded as

$$\begin{bmatrix} X^-(x_1,x_2) \\ Y^-(x_1,x_2) \\ Z^-(x_1,x_2) \\ D^-(x_1,x_2) \\ \Phi^-(x_1,x_2) \end{bmatrix} = \sum_{m=1}^{\infty}\sum_{n=1}^{\infty} \begin{bmatrix} X^-_{mn}\cos\left(\frac{m\pi x_1}{a}\right)\sin\left(\frac{n\pi x_2}{b}\right) \\ Y^-_{mn}\sin\left(\frac{m\pi x_1}{a}\right)\cos\left(\frac{n\pi x_2}{b}\right) \\ Z^-_{mn}\sin\left(\frac{m\pi x_1}{a}\right)\sin\left(\frac{n\pi x_2}{b}\right) \\ D^-_{mn}\sin\left(\frac{m\pi x_1}{a}\right)\sin\left(\frac{n\pi x_2}{b}\right) \\ \Phi^-_{mn}\sin\left(\frac{m\pi x_1}{a}\right)\sin\left(\frac{n\pi x_2}{b}\right) \end{bmatrix} \tag{28}$$

$$\begin{bmatrix} X^+(x_1,x_2) \\ Y^+(x_1,x_2) \\ Z^+(x_1,x_2) \\ D^+(x_1,x_2) \\ \Phi^+(x_1,x_2) \end{bmatrix} = \sum_{m=1}^{\infty}\sum_{n=1}^{\infty} \begin{bmatrix} X^+_{mn}\cos\left(\frac{m\pi x_1}{a}\right)\sin\left(\frac{n\pi x_2}{b}\right) \\ Y^+_{mn}\sin\left(\frac{m\pi x_1}{a}\right)\cos\left(\frac{n\pi x_2}{b}\right) \\ Z^+_{mn}\sin\left(\frac{m\pi x_1}{a}\right)\sin\left(\frac{n\pi x_2}{b}\right) \\ D^+_{mn}\sin\left(\frac{m\pi x_1}{a}\right)\sin\left(\frac{n\pi x_2}{b}\right) \\ \Phi^+_{mn}\sin\left(\frac{m\pi x_1}{a}\right)\sin\left(\frac{n\pi x_2}{b}\right) \end{bmatrix} \tag{29}$$

where

$$\begin{bmatrix} X^-_{mn} \\ Y^-_{mn} \\ Z^-_{mn} \\ D^-_{mn} \\ \Phi^-_{mn} \end{bmatrix} = \frac{4}{ab} \begin{bmatrix} \int_0^a\int_0^b X^-(x_1,x_2)\cos\left(\frac{m\pi x_1}{a}\right)\sin\left(\frac{n\pi x_2}{b}\right)\mathrm{d}x_1\,\mathrm{d}x_2 \\ \int_0^a\int_0^b Y^-(x_1,x_2)\sin\left(\frac{m\pi x_1}{a}\right)\cos\left(\frac{n\pi x_2}{b}\right)\mathrm{d}x_1\,\mathrm{d}x_2 \\ \int_0^a\int_0^b Z^-(x_1,x_2)\sin\left(\frac{m\pi x_1}{a}\right)\sin\left(\frac{n\pi x_2}{b}\right)\mathrm{d}x_1\,\mathrm{d}x_2 \\ \int_0^a\int_0^b D^-(x_1,x_2)\sin\left(\frac{m\pi x_1}{a}\right)\sin\left(\frac{n\pi x_2}{b}\right)\mathrm{d}x_1\,\mathrm{d}x_2 \\ \int_0^a\int_0^b \Phi^-(x_1,x_2)\sin\left(\frac{m\pi x_1}{a}\right)\sin\left(\frac{n\pi x_2}{b}\right)\mathrm{d}x_1\,\mathrm{d}x_2 \end{bmatrix} \tag{30}$$

$$\begin{bmatrix} X^+_{mn} \\ Y^+_{mn} \\ Z^+_{mn} \\ D^+_{mn} \\ \Phi^+_{mn} \end{bmatrix} = \frac{4}{ab} \begin{bmatrix} \int_0^a \int_0^b X^+(x_1,x_2) \cos\left(\frac{m\pi x_1}{a}\right) \sin\left(\frac{n\pi x_2}{b}\right) \mathrm{d}x_1\,\mathrm{d}x_2 \\ \int_0^a \int_0^b Y^+(x_1,x_2) \sin\left(\frac{m\pi x_1}{a}\right) \cos\left(\frac{n\pi x_2}{b}\right) \mathrm{d}x_1\,\mathrm{d}x_2 \\ \int_0^a \int_0^b Z^+(x_1,x_2) \sin\left(\frac{m\pi x_1}{a}\right) \sin\left(\frac{n\pi x_2}{b}\right) \mathrm{d}x_1\,\mathrm{d}x_2 \\ \int_0^a \int_0^b D^+(x_1,x_2) \sin\left(\frac{m\pi x_1}{a}\right) \sin\left(\frac{n\pi x_2}{b}\right) \mathrm{d}x_1\,\mathrm{d}x_2 \\ \int_0^a \int_0^b \Phi^-(x_1,x_2) \sin\left(\frac{m\pi x_1}{a}\right) \sin\left(\frac{n\pi x_2}{b}\right) \mathrm{d}x_1\,\mathrm{d}x_2 \end{bmatrix} \tag{31}$$

Substituting (17) and (18) into boundary conditions (15) and (16), with (28) and (29) being considered, we have

$$\begin{aligned} &X_{mn}(0) = X^-_{mn} \qquad Y_{mn}(0) = Y^-_{mn} \qquad Z_{mn}(0) = Z^-_{mn} \\ &D_{mn}(0) = D^-_{mn} \qquad (\text{or } \Phi_{mn}(0) = \Phi^-_{mn}) \end{aligned} \tag{32}$$

$$\begin{aligned} &X_{mn}(h) = \mathrm{e}^{-\alpha} X^+_{mn} \qquad Y_{mn}(h) = \mathrm{e}^{-\alpha} Y^+_{mn} \qquad Z_{mn}(h) = \mathrm{e}^{-\alpha} Z^+_{mn} \\ &D_{mn}(h) = \mathrm{e}^{-\alpha} D^+_{mn} \qquad (\text{or } \Phi_{mn}(h) = \Phi^+_{mn}) \end{aligned} \tag{33}$$

Substituting (32) and (33) into (27), we can solve these eight algebraic equations for eight unknowns, $U_{mn}(0)$, $V_{mn}(0)$, $W_{mn}(0)$, $\Phi_{mn}(0)$, $U_{mn}(h)$, $V_{mn}(h)$, $W_{mn}(h)$, $\Phi_{mn}(h)$. Hence, all the components of $\mathbf{M}_{mn}(\mathbf{0})$ are obtained. Eqs. (17), (18) and (23) can then be used to calculate exactly the coupling electroelastic field in the plate.

4. Numerical examples

In this section numerical study of FGPM square plate ($a = b = 1$ m, $h = 0.1$ m), which is simply supported and grounded on its four lateral edges, will be made based on the above exact solution. The material chosen for the study is PZT-4 that has the material properties at $x_3 = 0$, as follows (Cheng et al., 2000):

$$\begin{aligned} &c^0_{1111} = c^0_{2222} = 139 \text{ GPa}, \quad c^0_{3333} = 115 \text{ GPa}, \quad c^0_{1122} = 77.8 \text{ GPa}, \quad c^0_{1133} = c^0_{2233} = 74.3 \text{ GPa}, \\ &c^0_{2323} = c^0_{3131} = 25.6 \text{ GPa}, \quad c^0_{1212} = 30.6 \text{ GPa}, \quad e^0_{311} = e^0_{322} = -5.2 \text{ C/m}^2, \quad e^0_{333} = 15.1 \text{ C/m}^2, \\ &e^0_{113} = e^0_{223} = 12.7 \text{ C/m}^2, \quad \lambda^0_{11} = \lambda^0_{22} = 1.306 \times 10^4 \text{ pF/m}, \quad \lambda^0_{33} = 1.151 \times 10^4 \text{ pF/m} \end{aligned}$$

Numerical results are presented for four cases of sinusoidal loading for which only one term solution is needed ($m = n = 1$). The four cases considered here are:

Case 1:

$$Z^+(x_1,x_2) = -Z_0 \sin\left(\frac{\pi x_1}{a}\right) \sin\left(\frac{\pi x_2}{b}\right) \quad (Z_0 = 1 \text{ Pa})$$

$$Y^+(x_1,x_2) = X^+(x_1,x_2) = Z^-(x_1,x_2) = Y^-(x_1,x_2) = X^-(x_1,x_2) = D^+(x_1,x_2) = D^-(x_1,x_2) = 0.$$

Case 2:

$$Z^+(x_1,x_2) = -Z_0 \sin\left(\frac{\pi x_1}{a}\right) \sin\left(\frac{\pi x_2}{b}\right) \quad (Z_0 = 1 \text{ Pa})$$

$$Y^+(x_1,x_2) = X^+(x_1,x_2) = Z^-(x_1,x_2) = Y^-(x_1,x_2) = X^-(x_1,x_2) = \phi^+(x_1,x_2) = \phi^-(x_1,x_2) = 0$$

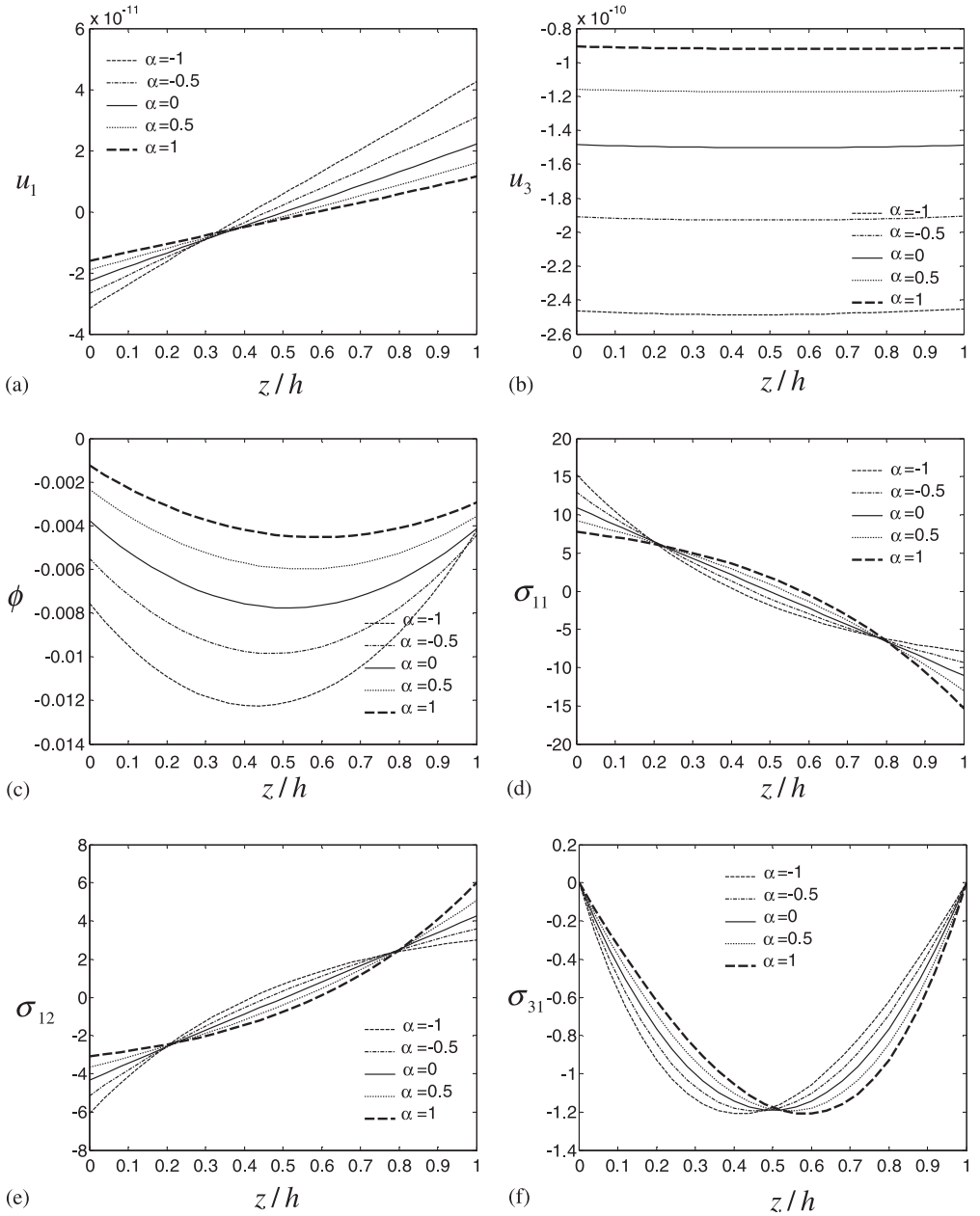

Fig. 2. Variation of physical quantities with coordinate x_3 at a location ($x_1/a = 1/4, x_2/b = 1/4$) for case 1: (a) in-plane displacement u_1 (m), (b) transverse displacement u_3 (m), (c) electric potential ϕ (V), (d) in-plane normal stress σ_{11} (Pa), (e) in-plane shear stress σ_{12} (Pa), (f) out-of-plane shear stress σ_{31} (Pa), (g) out-of-plane normal stress σ_{33} (Pa), (h) out-of-plane electric field E_3 (V/m), (i) in-plane electric field E_1 (V/m), (j) out-of-plane electric displacement D_3 (C/m^2) and (k) in-plane electric displacement D_1 (C/m^2).

Case 3:

$$D^+(x_1,x_2) = D^-(x_1,x_2) = D_0 \sin\left(\frac{\pi x_1}{a}\right)\sin\left(\frac{\pi x_2}{b}\right) \quad (D_0 = 1\times 10^{-6}\ \mathrm{C/m^2})$$

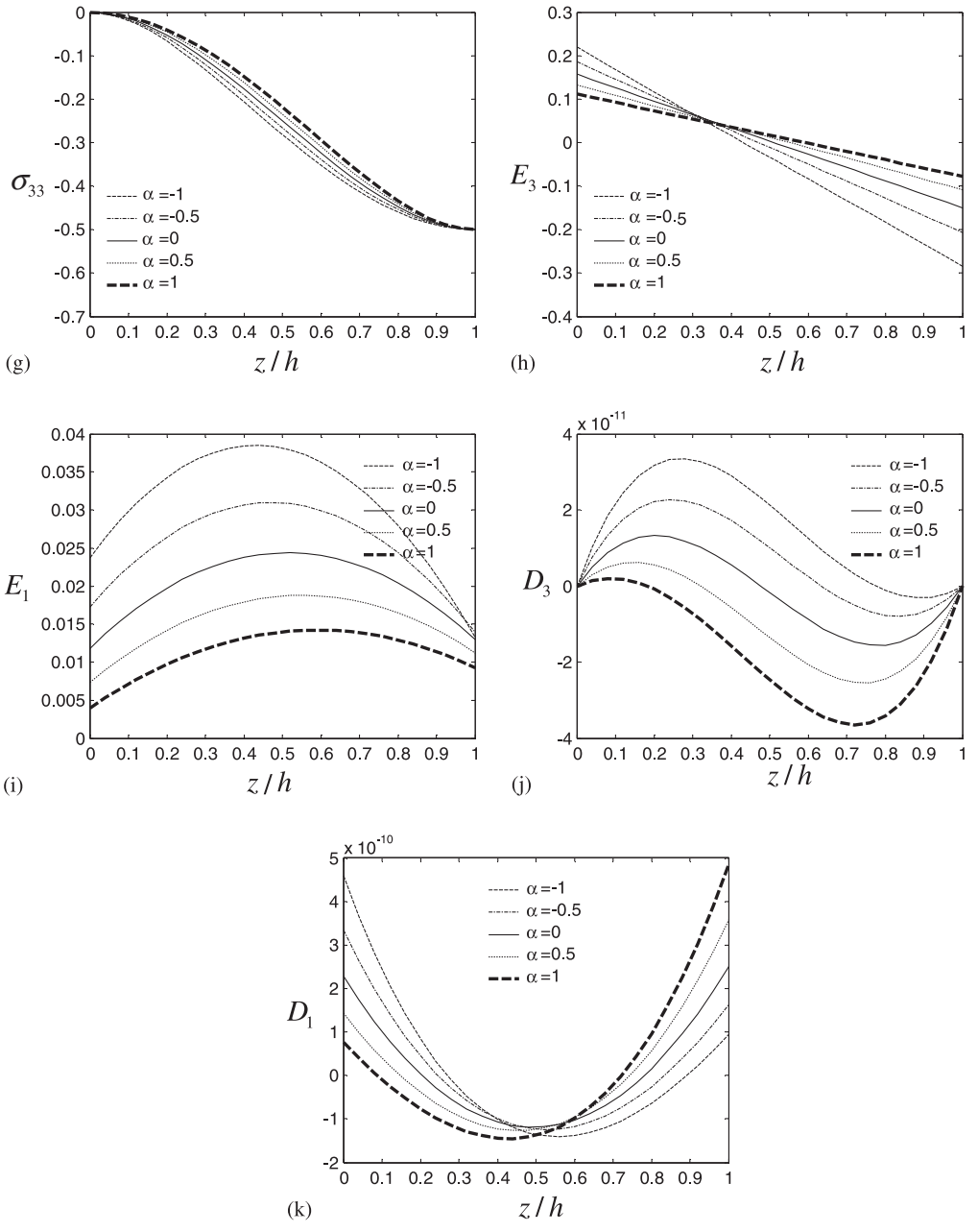

Fig. 2 (*continued*)

$$X^+(x_1,x_2) = Y^+(x_1,x_2) = Z^+(x_1,x_2) = X^-(x_1,x_2) = Y^-(x_1,x_2) = Z^-(x_1,x_2) = 0$$

Case 4:

$$\phi^+(x_1,x_2) = \phi_0 \sin\left(\frac{\pi x_1}{a}\right) \sin\left(\frac{\pi x_2}{b}\right) \quad (\phi_0 = 1 \text{ V})$$

$$X^+(x_1,x_2) = Y^+(x_1,x_2) = Z^+(x_1,x_2) = X^-(x_1,x_2) = Y^-(x_1,x_2) = Z^-(x_1,x_2) = \phi^-(x_1,x_2) = 0$$

The variation of displacements, u_1 and u_3, electric potential, ϕ, stresses, σ_{11}, σ_{12}, σ_{31} and σ_{33}, electric fields, E_3 and E_1, electric displacements, D_3 and D_1, as a function of the plate thickness coordinate x_3, at a

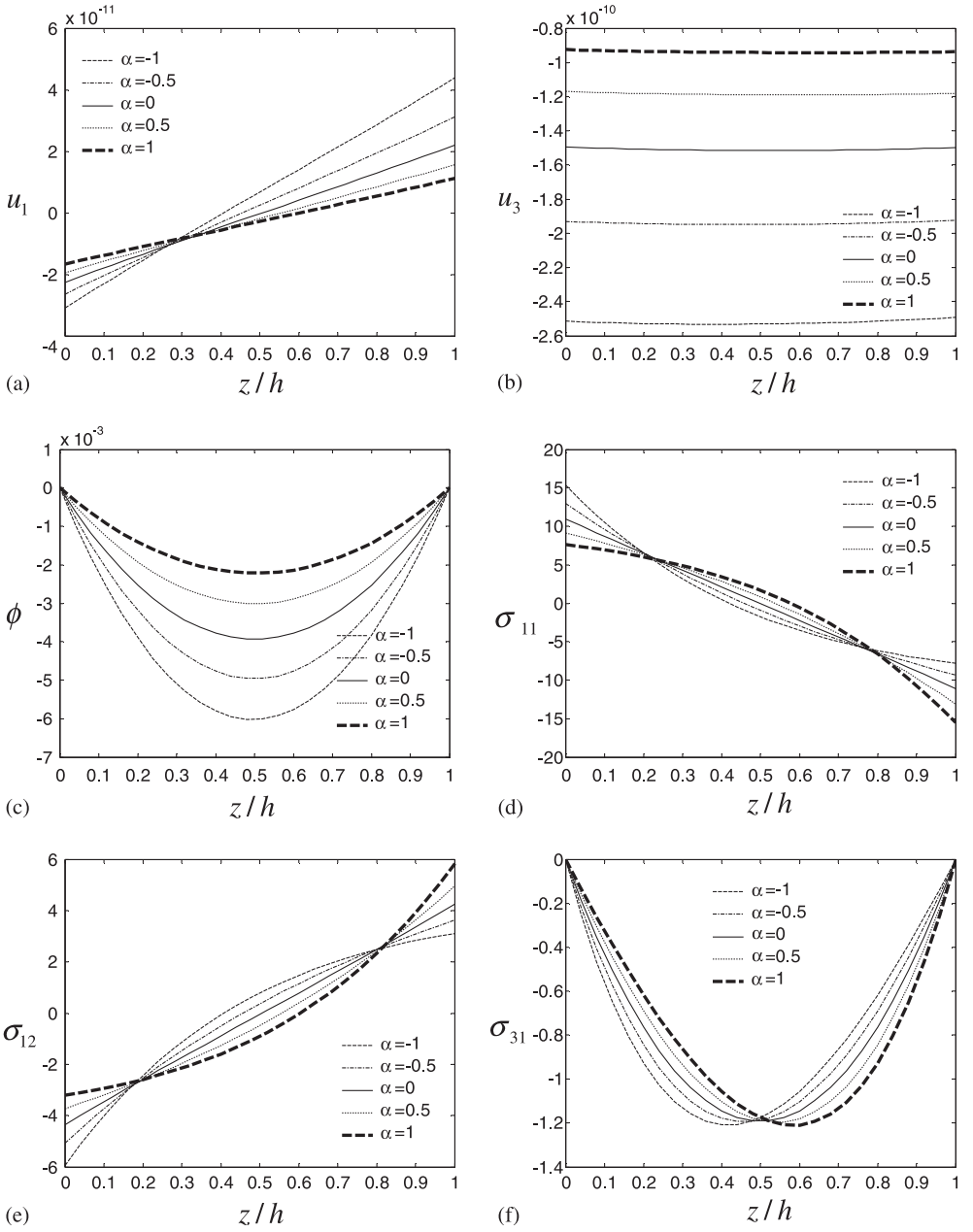

Fig. 3. Variation of physical quantities with coordinate x_3 at a location ($x_1/a = 1/4$, $x_2/b = 1/4$) for case 2: (a) in-plane displacement u_1 (m), (b) transverse displacement u_3 (m), (c) electric potential ϕ (V), (d) in-plane normal stress σ_{11} (Pa), (e) in-plane shear stress σ_{12} (Pa), (f) out-of-plane shear stress σ_{31} (Pa), (g) out-of-plane normal stress σ_{33} (Pa), (h) out-of-plane electric field E_3 (V/m), (i) in-plane electric field E_1 (V/m), (j) out-of-plane electric displacement D_3 (C/m^2) and (k) in-plane electric displacement D_1 (C/m^2).

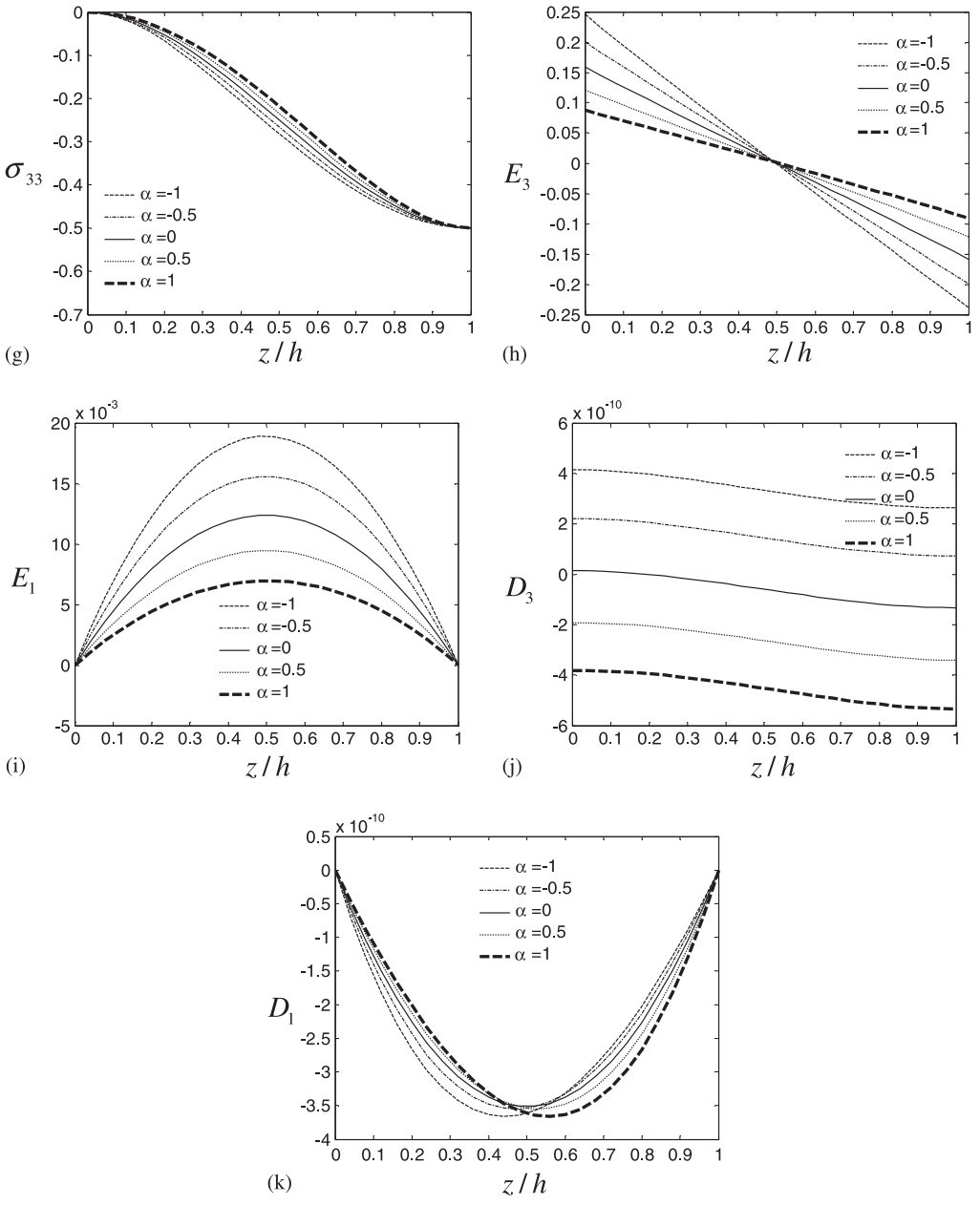

Fig. 3 (*continued*)

chosen field point ($x_1/a = 1/4$, $x_2/b = 1/4$), are shown in Figs. 2–5, respectively for cases 1–4. In these figures, the material property gradient index α is taken for five values: −1, −0.5, 0, 0.5, 1. The displacement u_2, stresses σ_{22} and σ_{32}, electric field E_2, electric displacement D_2 are not depicted since their distributions along the plate thickness direction are similar to those of u_1, σ_{11}, σ_{31}, E_1 and D_1, respectively, due to the symmetry of the problem. From these figures following observations can be made:

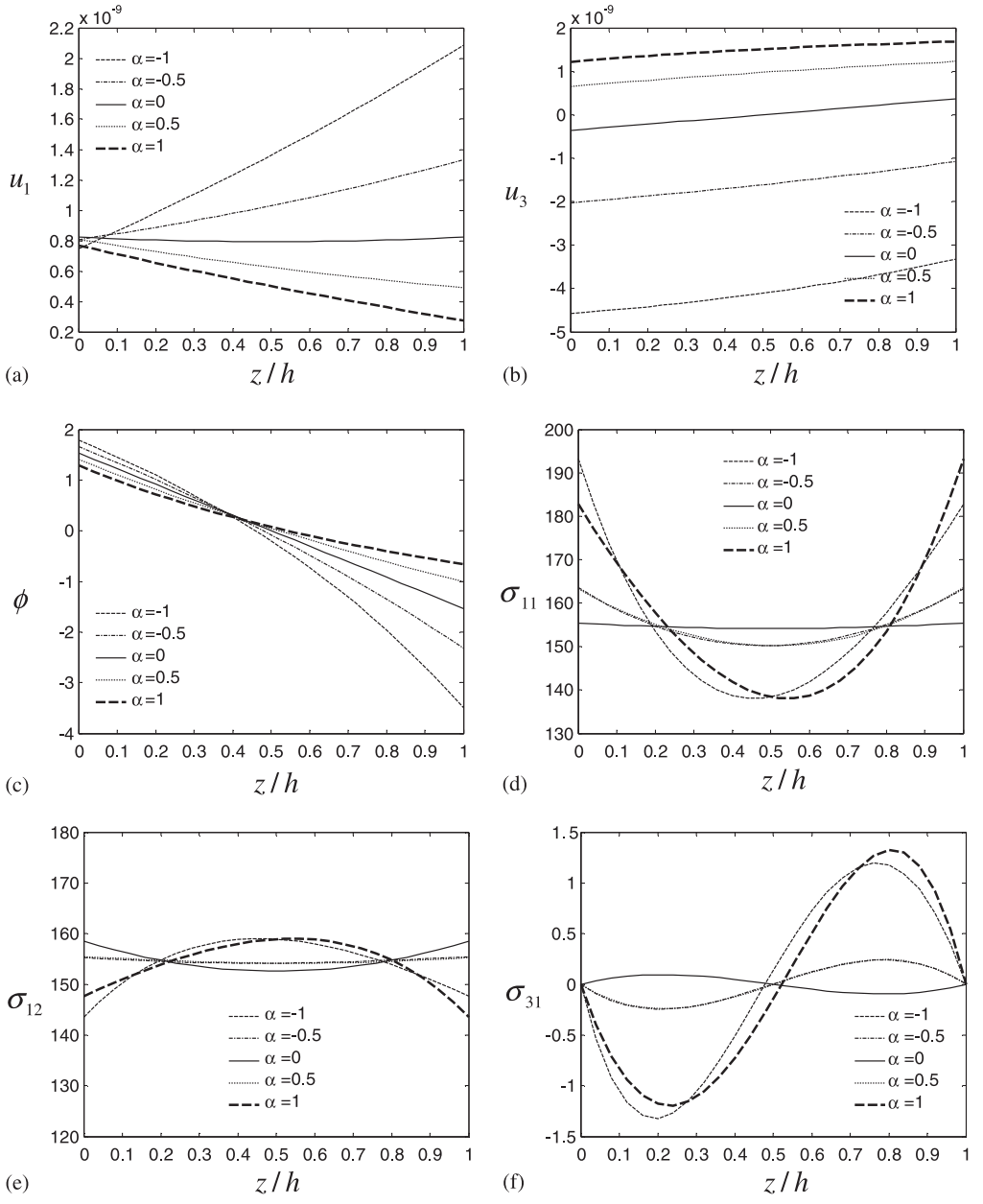

Fig. 4. Variation of physical quantities with coordinate x_3 at a location ($x_1/a = 1/4, x_2/b = 1/4$) for case 3: (a) in-plane displacement u_1 (m), (b) transverse displacement u_3 (m), (c) electric potential ϕ (V), (d) in-plane normal stress σ_{11} (Pa), (e) in-plane shear stress σ_{12} (Pa), (f) out-of-plane shear stress σ_{31} (Pa), (g) out-of-plane normal stress σ_{33} (Pa), (h) out-of-plane electric field E_3 (V/m), (i) in-plane electric field E_1 (V/m), (j) out-of-plane electric displacement D_3 (C/m^2) and (k) in-plane electric displacement D_1 (C/m^2).

(1) For pure mechanical loading (cases 1 and 2), it can be found from Figs. 2 and 3 that transverse displacement u_3 demonstrates essentially uniform distribution along the plate thickness direction, while in-plane displacements, u_1 and u_2, and out-of-plane electric field, E_3, show linear variations across the

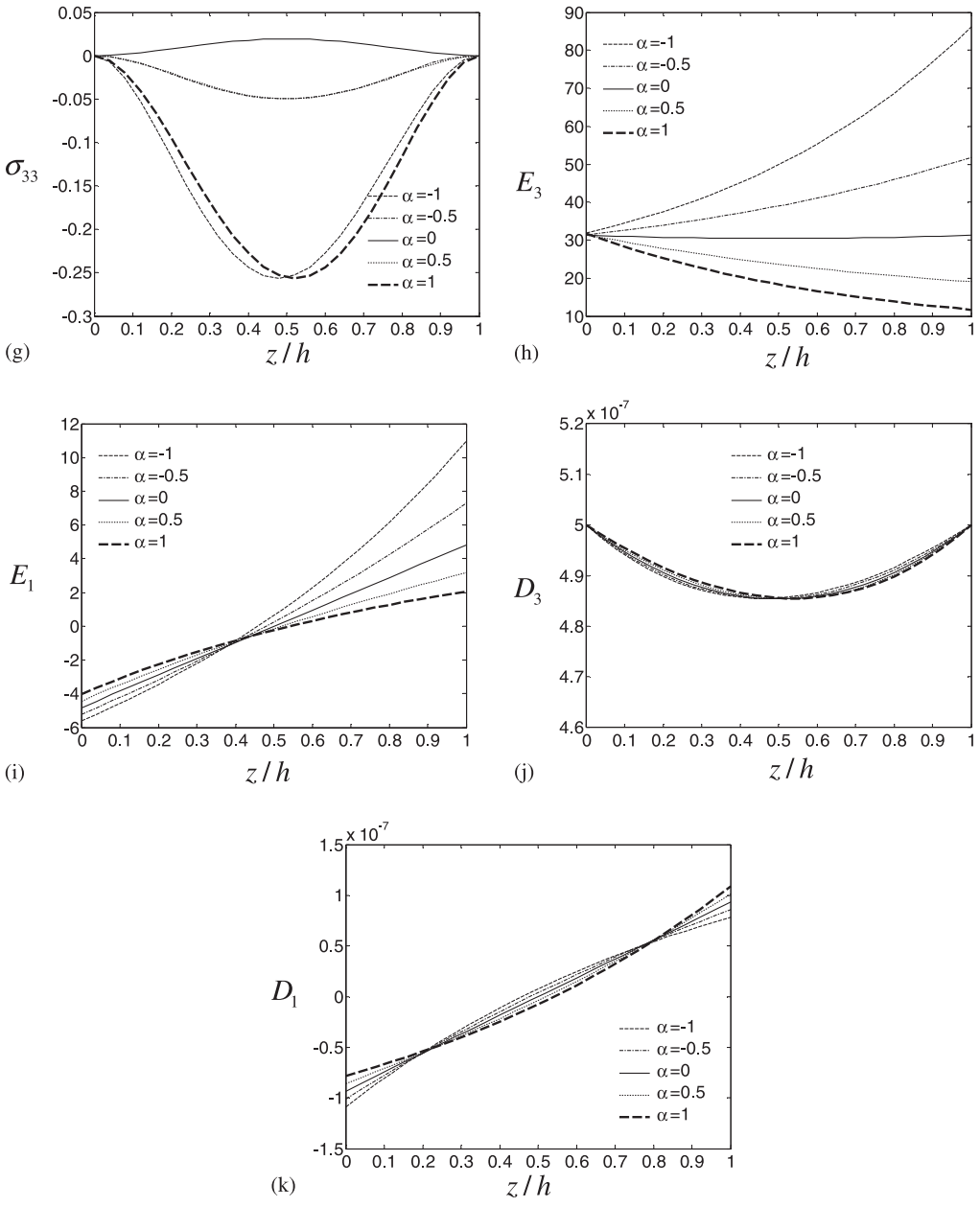

Fig. 4 (*continued*)

thickness of the plate. Furthermore, out-of-plane stresses, σ_{31}, σ_{32} and σ_{33}, in-plane electric fields, E_1 and E_2, and electric displacements D_1, D_2 and D_3 exhibit polynomial distributions. In contrast to the case of a homogeneous piezoelectric material (when $\alpha = 0$) where in-plane stresses σ_{11}, σ_{22} and σ_{12} are linear distribution over the thickness, these in-plane stress components are varied nonlinearly along the thickness direction for functionally gradient materials (when $\alpha \neq 0$).

(2) For pure electric loading (cases 3 and 4), several characteristics different from the cases of pure mechanical loading (cases 1 and 2) can be seen from Figs. 4 and 5. Firstly, transverse displacement u_3 is no longer uniform across the plate thickness. Secondly, in-plane displacements, u_1 and u_2, and out-of-plane

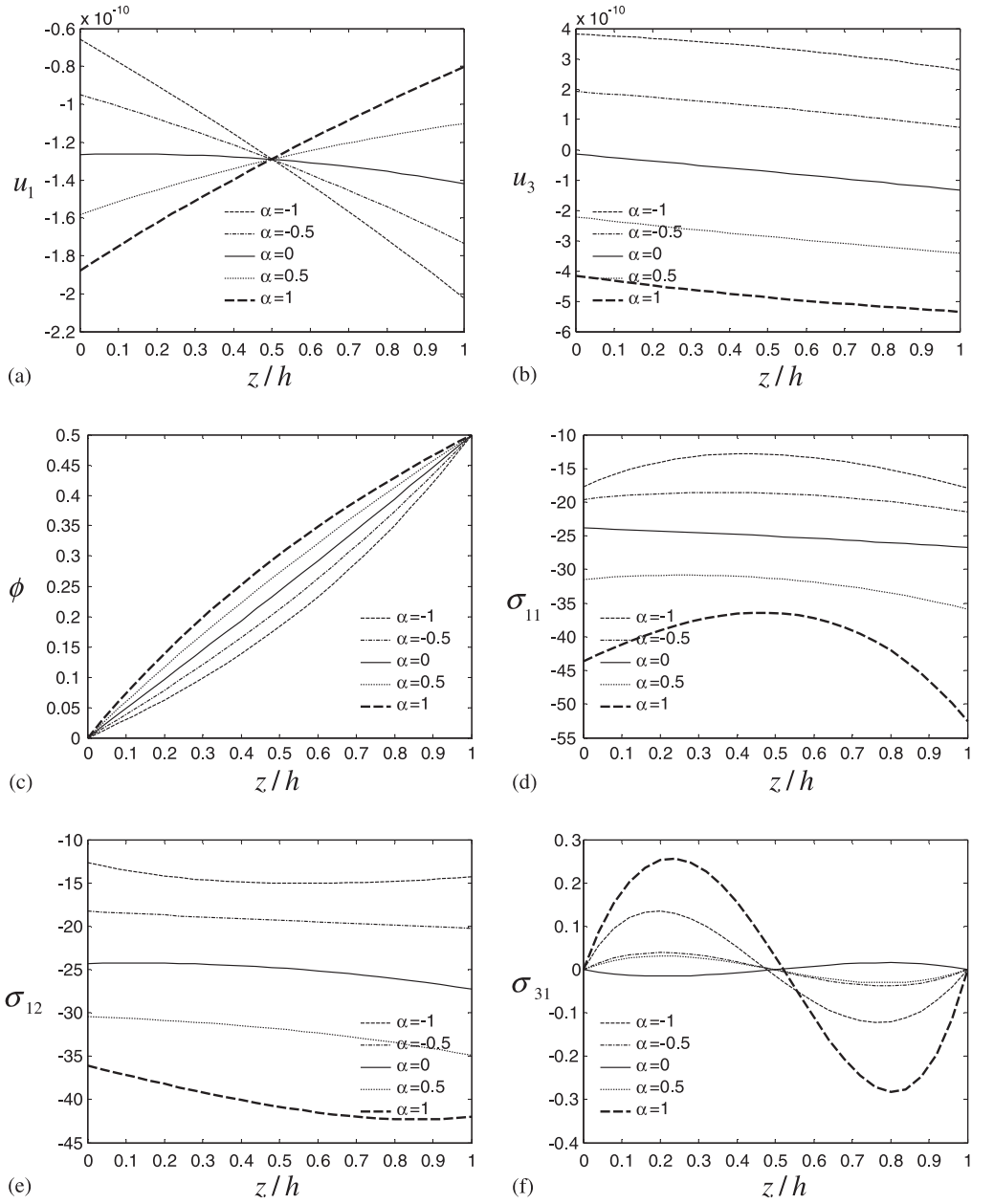

Fig. 5. Variation of physical quantities with coordinate x_3 at a location ($x_1/a = 1/4, x_2/b = 1/4$) for case 4: (a) in-plane displacement u_1 (m), (b) transverse displacement u_3 (m), (c) electric potential ϕ (V), (d) in-plane normal stress σ_{11} (Pa), (e) in-plane shear stress σ_{12} (Pa), (f) out-of-plane shear stress σ_{31} (Pa), (g) out-of-plane normal stress σ_{33} (Pa), (h) out-of-plane electric field E_3 (V/m), (i) in-plane electric field E_1 (V/m), (j) out-of-plane electric displacement D_3 (C/m^2) and (k) in-plane electric displacement D_1 (C/m^2).

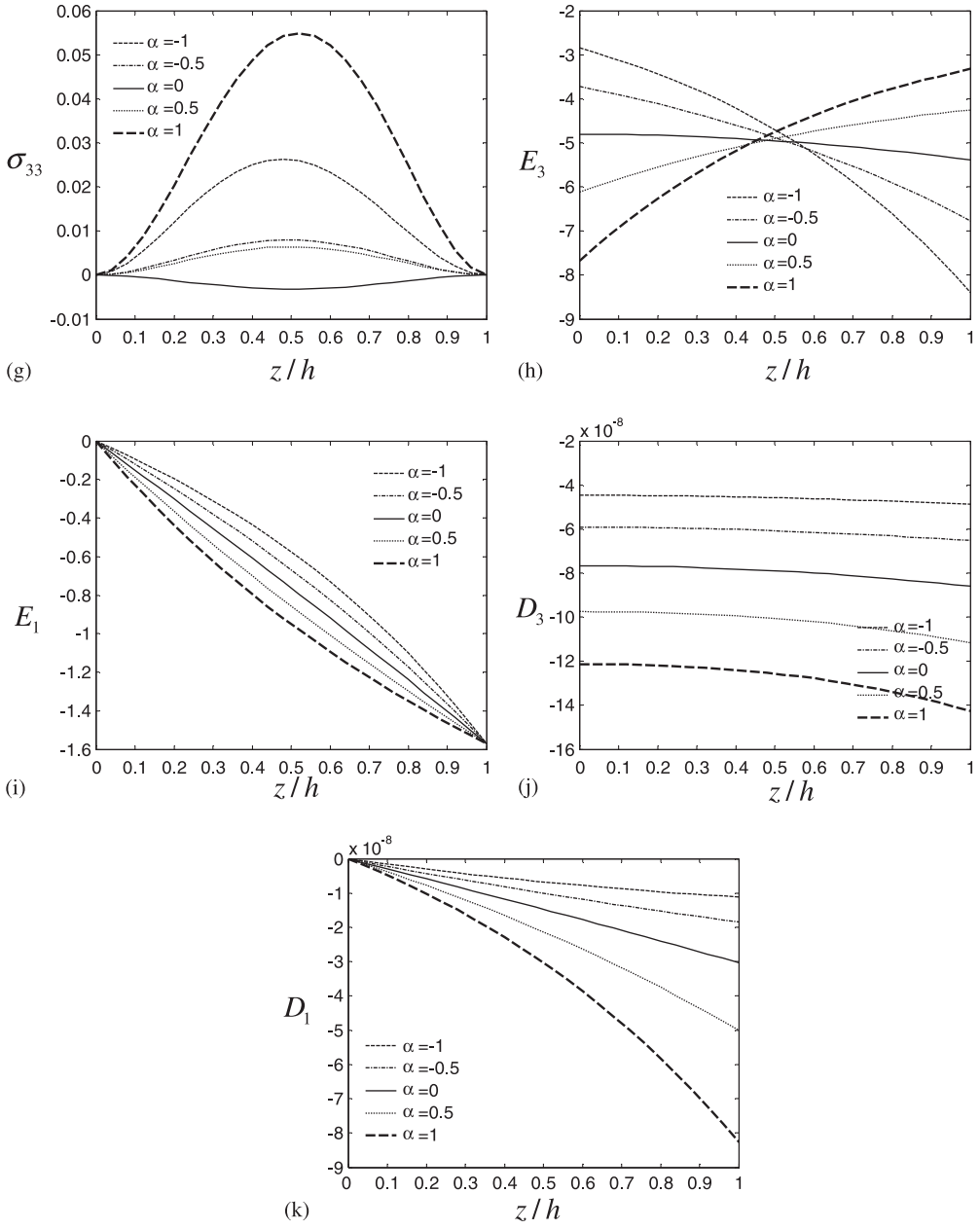

Fig. 5 (*continued*)

electric field, E_3, become nonlinear distributions over the thickness for functionally gradient materials ($\alpha \neq 0$) as compared to a linear distribution for a homogeneous piezoelectric material ($\alpha = 0$). Finally, it is interesting to note that for different functionally gradient index α, electric displacements D_1, D_2 (similar to D_1 and not depicted for brevity) and D_3 take almost the same values in case 3, while they have large differences in case 4.

(3) For all four cases of loading considered here, out-of-plane stresses (σ_{13}, σ_{23} and σ_{33}) are negligible compared to in-plane stresses (σ_{11} and σ_{22}), which constitutes a basic assumption in most classical plate theories. Moreover, in-plane electric fields (E_1 and E_2) are also negligible compared to out-of-plane electric field (E_3).

Above observations may be useful for establishing a simplified two-dimensional FGPM plate theory. For example, the constant distribution of transverse displacement and the linear variation of in-plane displacements and the out-of-plane electric field, across the plate thickness are good approximations for the FGPM plate under pure mechanical loading, but these assumptions may be invalid for the case of pure electric loading or coupling mechanical-electric loading. This means that more exact assumptions should be made when a simplified two-dimensional FGPM plate theory is constructed, applicable to general cases with both the mechanical and electric loading.

5. Concluding remarks

An exact three-dimensional solution is obtained for a FGPM rectangular plate simply supported and grounded along its four edges by means of the state space approach. The mechanical and electric properties of the material were assumed to have the same exponent-law dependence on the thickness-coordinate of the plate. The obtained solution is valid for arbitrary mechanical and electric loads applied on the upper and lower surfaces of the plate and can play as a benchmark result when establishing simplified FGPM plate theories or assessing approximate computational models for FGPM plates.

Acknowledgements

This work was supported by the National Natural Science Foundation of China (nos. 10072041 and 10125209) and the Teaching and Research Award Fund for Outstanding Young Teachers in High Education Institutions of MOE, PR China.

References

Chen, W.Q., Ding, H.J., 2002. On free vibration of a functionally graded piezoelectric rectangular plate. Acta Mech. 153, 207–216.

Cheng, Z.Q., Lim, C.W., Kitipornchai, S., 2000. Three-dimensional asymptotic approach to inhomogeneous and laminated piezoelectric plates. Int. J. Solids Struct. 37, 3153–3175.

Delale, F., Erdogan, F., 1988. On the mechanical modeling of the interfacial region in bonded half planes. ASME J. Appl. Mech. 55, 317–324.

Ding, H.J., Xu, R.Q., Chi, Y.W., Chen, W.Q., 1999. Free axisymmetric vibration of transversely isotropic piezoelectric circular plates. Int. J. Solids Struct. 36, 4629–4652.

Erdogan, F., 1985. The crack problem for bonded nonhomogeneous materials under antiplane shear loading. ASME J. Appl. Mech. 52, 823–828.

Gandhi, M.V., Thompson, B.S., 1992. Smart Materials and Structures. Chapman & Hall, London.

Gantmacher, F.R., 1960. The Theory of Matrix. Chelsea, New York.

Gu, P., Asaro, J., 1997. Crack in functionally graded materials. Int. J. Solids Struct. 34, 1–17.

Hu, K.Q., Zhong, Z., Jin, B., 2002. Anti-plane shear crack in a functionally gradient piezoelectric material. Acta Mech. Solida Sin. 15, 140–148.

Jin, B., Zhong, Z., 2002. A moving mode-III crack in functionally graded piezoelectric material: permeable problem. Mechanics Research Communications 29, 217–224.

Lee, J.S., Jiang, L.Z., 1996. Exact electroelastic analysis of piezoelectric laminae via state space approach. Int. J. Solids Struct. 33, 977–990.

Li, C., Weng, G.J., 2002a. Yoffer-type moving crack in a functionally graded piezoelectric material. Proc. R. Soc. Lond. A. 458, 381–399.

Li, C., Weng, G.J., 2002b. Antiplane crack problem in functionally graded piezoelectric materials. ASME J. Appl. Mech. 69, 481–488.

Lim, C.W., He, L.H., 2001. Exact solution of a compositionally graded piezoelectric layer under uniform stretch, bending and twisting. Int. J. Mech. Sci. 43, 2479–2492.

Liu, G.R., Tani, J., 1994. Surface waves in functionally gradient piezoelectric plates. ASME J. Vib. Acoust. 116, 440–448.

Maugin, G.A., 1988. Continuum Mechanics of Electromagnetic Solids. North-Holland, Amsterdam.

Noda, N., Jin, Z.H., 1993. Thermal stress intensity factors for a crack in a strip of a functionally gradient material. Int. J. Solids Struct. 30, 1039–1056.

Rao, S.S., Sunar, M., 1994. Piezoelectricity and its use in disturbance sensing and control of flexible structures: A survey. Appl. Mech. Rev. 47, 113–123.

Reddy, J.N., Cheng, Z.Q., 2001. Three-dimensional solutions of smart functionally graded plates. ASME J. Appl. Mech. 68, 234–241.

Shelley II, W.F., Wan, S., Bowman, K.J., 1999. Functionally graded piezoelectric ceramics. Mater. Sci. Forum 308–311, 515–520.

Tiersten, H.F., 1969. Linear Piezoelectric Plate Vibrations. Plenum Press, New York.

Wu, C.C.M., Kahn, M., Moy, W., 1996. Piezoelectric ceramics with functional gradients: a new application in material design. J. Am. Ceram. Soc. 79, 809–812.

Zhu, X.H., Meng, Z.Y., 1995. Operational principle, fabrication and displacement characteristic of a functionally gradient piezoelectric ceramic actuator. Sensor and Actuator. 48, 169–176.